JACS
JOURNAL OF THE AMERICAN CHEMICAL SOCIETY
pubs.acs.org/JACS
Article

Phase-Migrating Z-Scheme Charge Transportation Enables Photoredox Catalysis Harnessing Water as an Electron Source

Ren Itagaki, Akinobu Nakada,* Hajime Suzuki, Osamu Tomita, Ho-Chol Chang,* and Ryu Abe*

Cite This: https://doi.org/10.1021/jacs.5c02276
Read Online

ABSTRACT: Z-schematic photocatalytic reactions are of considerable interest because of their potential for application to reductive molecular conversions to value-added chemicals using water as an electron source. However, most demonstrations of Z-scheme photocatalysis have been limited to overall water splitting. In particular, it has been basically impossible to couple the reduction of "water-insoluble compounds" with water oxidation by conventional Z-scheme systems in aqueous solution. In this work, an unconventional Z-scheme electron transportation system with a "phase-migrating" redox mediator is constructed that enables photocatalytic conversion of water-insoluble compounds by using water as an electron/proton source. In a dichloroethane (DCE)/water biphasic solution, a molecular Ir(III) complex acts as a photoredox catalyst for the reductive coupling of benzyl bromide by using ferrocene (Fc) as an electron donor in the DCE phase. On the other side, an aqueous dispersion of a Bi_4TaO_8Cl semiconductor loaded with a $(Fe,Ru)O_x$ cocatalyst photocatalyzed water oxidation using ferrocenium (Fc^+) as an electron acceptor. Because the partition coefficients of Fc^+/Fc are significantly different, the Fc^+ and Fc generated by photoinduced electron transfer in each reaction could be selectively extracted to the opposite liquid phase. Spontaneous phase migration enables direction-selective electron transport across the organic/water interface that connects the reduction and oxidation reactions in the separated reaction phase. Eventually, photocatalytic reductive conversion of "water-insoluble" organic compounds using "water as the electron/proton source" was demonstrated through the step-by-step Z-scheme photocatalysis with the phase-migrating Fc^+/Fc electron transportation.

INTRODUCTION

Photocatalytic molecular conversion by harnessing solar energy to generate chemical resources is of great interest, as can be seen in extensive studies on H_2 production,[1−4] CO_2 reduction,[5−9] and organic molecular transformations.[10−14] However, many reported photocatalytic reductive molecular conversion reactions require sacrificial electron donors. Replacing the sacrificial electron donor to use water as an electron source to drive such photocatalytic molecular conversion reactions is highly desirable from the viewpoint of solar energy conversion (i.e., positive Gibbs free energy changes in the total reaction)[2,3] and atom economy.[15]

The Z-scheme photocatalytic system, inspired by natural photosynthesis, has been developed as an effective strategy to connect reductive molecular conversion (e.g., H_2 production[1,3] and CO_2 reduction[9]) and water oxidation (Figure 1a). In this system, two different photocatalysts are employed for the reduction and water oxidation reactions, respectively, and an electron mediator plays an important role in transporting electrons from the oxidation photocatalyst to the reduction photocatalyst. Specifically, an O_2-evolving photocatalyst oxidizes water via photogenerated holes while supplying photoexcited electrons to the electron mediator. The electron mediator transports electrons to the second photocatalyst for the reductive reaction. In principle, the Z-scheme concept has great potential for application in various valuable molecular conversion reactions using water as the electron source. However, despite this potential, Z-scheme photocatalysis with electron mediators has been limited to overall water splitting[1,3,4] and a few examples of direct CO_2 reduction.[16] For instance, it would be attractive if reductive photoredox catalysis for organic molecular transformations could be achieved using water as an electron/proton source.

However, there are several challenges in achieving Z-scheme photoredox catalysis coupled with water oxidation: solubility and undesirable oxidation of the reaction substrate by the water oxidation photocatalyst (Figure 1b). Most photoredox catalysis has been carried out in organic solution[10,11,17] because

Received: February 6, 2025
Revised: April 8, 2025
Accepted: April 9, 2025

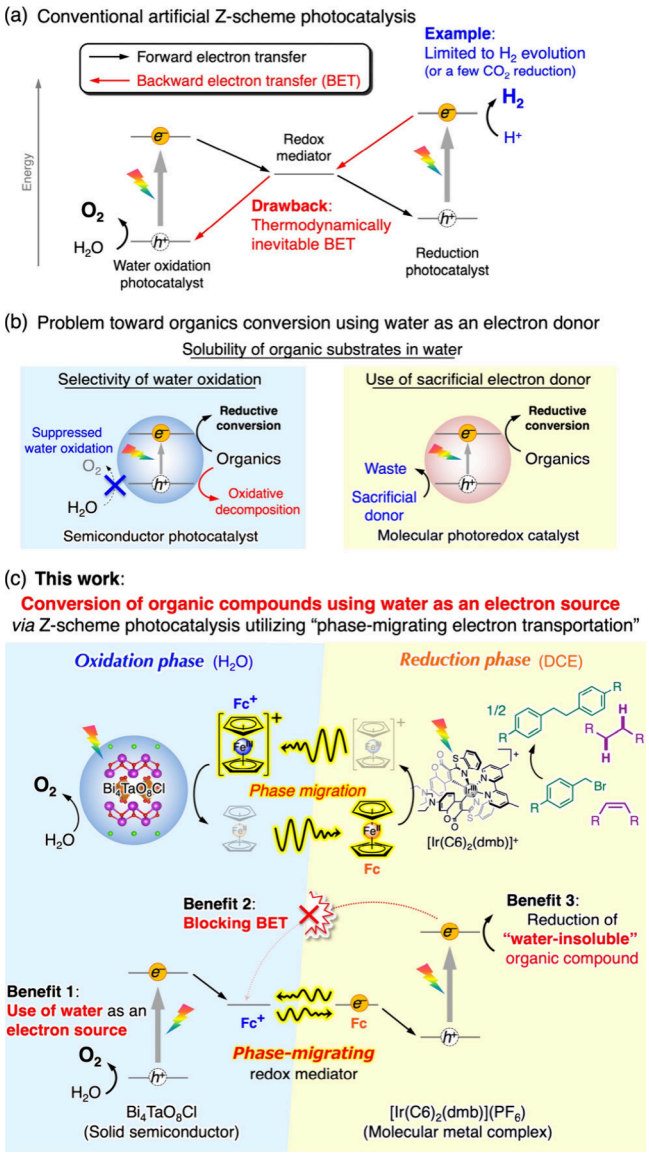

Figure 1. (a) General mechanism and drawbacks of Z-scheme photocatalysis. (b) Problem with photocatalytic reduction of organics using water as an electron source. (c) Z-scheme phase-migrating electron transport between two immiscible solutions developed in this work; this system enables the reductive conversion of water-insoluble organic compounds using water as the electron source.

of the limited solubility of organic compounds in water. In addition, oxidative decomposition and the conversion of organic compounds by semiconductor photocatalysts have been widely demonstrated,[18−20] indicating that undesirable oxidation of the reaction substrate by the water-oxidation photocatalyst must be suppressed in photoredox applications. Furthermore, backward charge transfer between the electron mediator and the photocatalyst is a common drawback in Z-scheme photocatalysis, irrespective of the type of reaction.[21] Hence, it is difficult to replace the sacrificial electron donor with water in photoredox catalysis by using conventional methods.

To overcome these drawbacks, this article describes a strategy to separate the reaction fields for photocatalytic reduction/oxidation using two immiscible water/organic solutions (Figure 1c). The use of biphasic solutions should enable the reduction/oxidation reaction fields to be separated and allow the reduction of "water-insoluble" organic compounds and water oxidation to proceed independently in the organic and aqueous phases, respectively. To connect the reduction/oxidation reactions that are separated in the biphasic system, a redox mediator that can transport electrons in a directionally selective migration between the two liquid phases upon photoinduced electron transfer is introduced. Liquid−liquid phase migration due to drastic changes in the partition coefficient by electron transfer is a key property of the phase-migrating electron mediator, of which the studies have been demonstrated by electrochemical techniques.[22,23] Regarding the application of photochemical molecular conversion, only a few examples of phase migration triggered by photoinduced electron transfer have been reported for quinones,[24] alkyl viologens,[25] and ferrocene.[26] However, all except one example are still sacrificial reactions without recovering the electron donor. Fukuzumi and co-workers reported the only example of nonsacrificial Z-scheme photocatalysis for water splitting in a biphasic toluene−H_2O solution.[24] An enhancement of water splitting activity was reported for a $SrTiO_3$ photocatalyst utilizing a phase boundary.[27] However, the application is still limited to water splitting; Z-scheme photocatalysis coupling reductive organic molecular conversion and water oxidation has never been established.

In this study, we constructed a Z-schematic photocatalytic system to connect photoredox catalysis and water oxidation with the biphasic solution and the phase-migrating ferrocenium/ferrocene (Fc^+/Fc) electron mediator. As an important key to achieving this challenging reaction, we first developed a photocatalytic system for water oxidation using Fc^+ as the electron acceptor to recycle Fc, which can be used as a reductant for photoredox catalysis in the organic phase. In the water oxidation reaction with Fc^+ as the electron acceptor, we employed and specially improved a particulate semiconductor Bi_4TaO_8Cl that has been developed as a heterogeneous photocatalyst for water splitting, the research field of which is completely different from photoredox catalysis in homogeneous solutions of molecular photocatalysts. Subsequently, the generated Fc was utilized as a recyclable electron donor for photocatalytic organic molecular conversion with the regeneration of Fc^+ in the aqueous phase by using a molecular Ir(III) complex $[Ir(C6)_2(dmb)](PF_6)$ as a photoredox catalyst. The direction-regulated electron transport by the Fc^+/Fc phase-migratable redox mediator connected these two distinct photocatalytic reactions, achieving photocatalytic reductive conversions of water-insoluble organics using water as the electron source (Figure 1c).

RESULTS AND DISCUSSION

Photocatalytic Water Oxidation Using Ferrocenium as an Electron Acceptor. To the best of our knowledge, Fc^+ has not been used as an electron acceptor in photocatalytic water oxidation. Because the electron mediator must be stable under the operating conditions, we investigated the stability of Fc^+ against O_2 and photoirradiation in aqueous solutions prior to the photocatalysis study (Figure S1). Under an Ar atmosphere, Fc^+ was stable in water without any additives (Figure S1a; pH 4.1). However, the characteristic absorption peak of Fc^+ at 620 nm decreased gradually in the presence of air (Figure S1b). Degradation was accelerated in a basic solution (Figure S1c; pH 11.6, adjusted with NaOH), whereas

https://doi.org/10.1021/jacs.5c02276
J. Am. Chem. Soc. XXXX, XXX, XXX−XXX

the absorption band of Fc^+ remained almost unchanged upon the addition of HCl, which decreased the pH to 2.5, even in air (Figure S1d). Similar stabilization was observed upon the addition of HNO_3 or H_2SO_4 at pH 2.5 (Figure S1e,f). In contrast, the addition of NaCl (pH 4.1) was not effective for stabilization (Figure S1g); therefore, the solution pH, rather than the presence of the Cl^- anion, is important for the stabilization of Fc^+ in the presence of air. Importantly, the UV−vis absorption of Fc^+ was almost unchanged in HCl solution (pH 2.5), even under visible-light (λ = 430 nm) irradiation (Figure S1h). Therefore, we can conclude that acidic conditions (pH 2.5) are suitable for the stable operation of Fc^+ as an electron acceptor for photocatalytic water oxidation to generate O_2. The subsequent photocatalytic reactions were carried out using aqueous Fc^+ solutions adjusted to pH 2.5 with HCl.

A bismuth-based layered oxyhalide, Bi_4TaO_8Cl,[28] was employed as the water oxidation photocatalyst. Single-phase Bi_4TaO_8Cl was synthesized from Bi_2O_3, Ta_2O_5, and BiOCl using a flux method[29] in NaCl/CsCl molten salt at 1023 K (Figure S2). Plate-like particles of Bi_4TaO_8Cl with dimensions of approximately 1 μm were observed in the scanning electron microscopy (SEM) image (Figure S3). An $(Fe,Ru)O_x$ species[30] as a cocatalyst was loaded onto the surface of Bi_4TaO_8Cl (Figures S4 and S5). Bi_4TaO_8Cl exhibits visible-light absorption up to approximately 480 nm (Figure 2a) with a

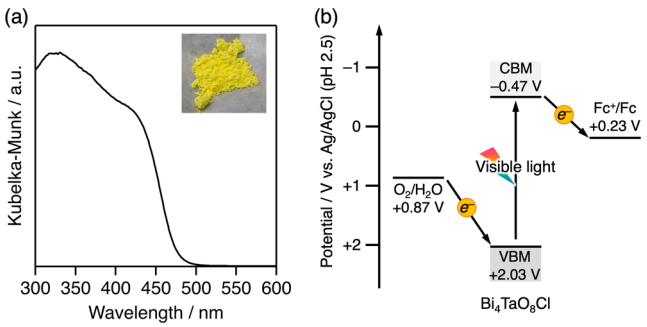

Figure 2. (a) UV−visible diffuse reflectance spectrum and (b) energy diagrams of Bi_4TaO_8Cl for photochemically oxidizing water using Fc^+ as an electron acceptor.

suitable conduction band potential (−0.47 V vs Ag/AgCl at pH 2.5) for reducing Fc^+ (0.23 V) and a valence band potential (2.03 V) for oxidizing water (0.87 V) (Figure 2b; see also Supporting Information for details, Figures S6−S8 and Table S1).

Photocatalytic water oxidation was carried out by irradiating an aqueous suspension of $(Fe,Ru)O_x$-loaded Bi_4TaO_8Cl with visible light (λ = 430 nm) in the presence of Fc^+Cl^- (1 mM, pH 2.5) under an Ar atmosphere. As shown in Figure 3a, the O_2 gas is rapidly generated using $(Fe,Ru)O_x$-loaded Bi_4TaO_8Cl, and its generation is saturated at 1.25 μmol within 30 min. The saturation amount corresponds to one-fourth of the consumption of the input Fc^+ electron acceptor (5 μmol), as seen from the UV−vis absorption changes in the reaction solution before and after photocatalysis (Figure S9b). Simultaneously, a corresponding amount of Fc was observed in the dichloroethane extract of the aqueous reaction solution (Figure S9c). In the absence of Fc^+ or photoirradiation, no O_2 evolved over $(Fe,Ru)O_x$-loaded Bi_4TaO_8Cl (Figures S10 and S11). Therefore, the overall reaction can be described as a photocatalytic water oxidation using Fc^+ as an electron acceptor, as shown in Figure 3c and eq 1.

$$H_2O + 2Fc^+ \xrightarrow{(Fe,Ru)O_x/Bi_4TaO_8Cl/h\nu\ (=430\ nm)} \frac{1}{2}O_2 + 2Fc + 2H^+ \quad (1)$$

Although single RuO_x or FeO_x modifications to bismuth-based oxyhalide semiconductors are also known to accelerate water oxidation by using the Fe(III) ion or IO_3^- as an electron acceptor,[30−32] unloaded or RuO_x- or FeO_x-loaded Bi_4TaO_8Cl did not generate O_2 when Fc^+ was used as the electron acceptor (Figures 3b and S12−S14). In these cases, strangely, Fc^+ was almost completely consumed, and Fc was generated to some extent, indicating that Fc^+ reduction occurred even without counterpart water oxidation. Notably, the amount of Fc generated was significantly lower than the amount of Fc^+ consumed (5 μmol) using unloaded or RuO_x- or FeO_x-loaded Bi_4TaO_8Cl, in contrast to the case of $(Fe,Ru)O_x$-loaded Bi_4TaO_8Cl (Figure 3b).

(Photo)electrochemical measurements of the Bi_4TaO_8Cl-based electrodes provided mechanistic insights into the role of the cocatalyst in photocatalytic water oxidation with an Fc^+ electron acceptor (Figure 4). The n-type Bi_4TaO_8Cl electrode showed cathodic responses without photoirradiation in the presence of Fc^+ (Figure 4a−c) and photoanodic responses in either the absence or presence of Fc^+ (Figure 4d−f). The cathodic responses show that cocatalyst loading positively shifts the catalytic onset potentials for the reduction of Fc^+ with respect to that of the pristine Bi_4TaO_8Cl electrode (Figure 4c), indicating that they facilitate the reduction of Fc^+ (Figure 4a). In particular, $(Fe,Ru)O_x$ loading resulted in the greatest shift in the catalytic onset and thus accelerated the reduction of Fc^+ most effectively. On the other hand, the Bi_4TaO_8Cl-based electrodes exhibited photoanodic responses under irradiation of intermittent visible light (λ = 430 nm). The magnitude of the photoanodic responses to water oxidation in the absence of Fc^+ followed the order $(Fe,Ru)O_x \approx RuO_x > FeO_x >$ unloaded Bi_4TaO_8Cl (Figure 4e). As previously reported, the enhanced currents by $(Fe,Ru)O_x$ and RuO_x modification were derived from the effective capture of photogenerated holes and accelerated water oxidation catalysis.[30] Such bifunctional roles of the RuO_x-based cocatalyst on facilitating water oxidation and reduction of redox mediators (e.g., Fe^{3+} and IO_3^-) have also been reported previously.[33−35]

More importantly, the addition of Fc^+ resulted in contrasting photoanodic responses (Figure 4f). For the unloaded and FeO_x- and RuO_x-loaded Bi_4TaO_8Cl electrodes, the presence of Fc^+ significantly increased the anodic photocurrent due to the oxidation of Fc^+. The competition for excessive oxidation (decomposition) of Fc^+ causes the deactivation of photocatalytic water oxidation in the cases of unloaded and FeO_x- or RuO_x-loaded Bi_4TaO_8Cl (Figure S15), leading to the generation of Fc without forming O_2 (Figure 3b). In contrast, the undesirable oxidation of Fc^+ was significantly suppressed by the loading of the $(Fe,Ru)O_x$ cocatalyst (Figure 4f), leading to the selective oxidation of water with the stoichiometric formation of Fc (Figure 3b).

One can notice that the peak position of Ru-3d XPS, which reflects the valence state of the Ru component, was slightly different between loaded RuO_x and $(Fe,Ru)O_x$ species (Figure S4). Extended X-ray absorption fine structure (EXAFS) provided further insights into the structural differences of

https://doi.org/10.1021/jacs.5c02276
J. Am. Chem. Soc. XXXX, XXX, XXX−XXX

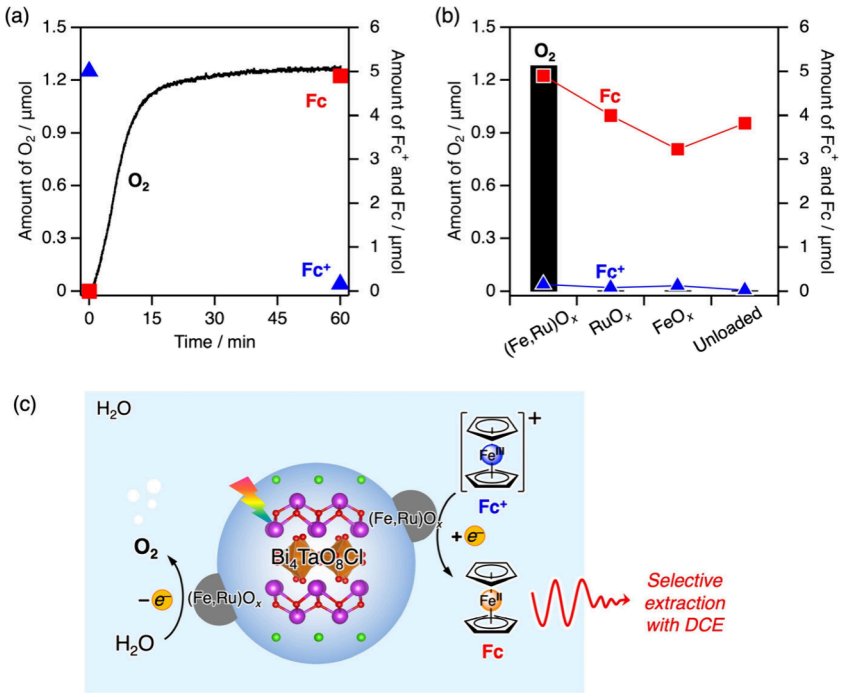

Figure 3. (a) Time course of O_2 and Fc formation along with Fc^+ conversion using $(Fe,Ru)O_x$-loaded Bi_4TaO_8Cl photocatalysts in an aqueous solution (5 mL) containing 1.0 mM Fc^+ (pH 2.5 adjusted with HCl) as an electron acceptor under visible-light irradiation (λ = 430 nm). (b) Comparison of the photocatalytic activities for O_2 and Fc formation along with the conversion of Fc^+ using $(Fe,Ru)O_x$-, RuO_x-, and FeO_x-loaded or unloaded Bi_4TaO_8Cl photocatalysts after irradiation with visible light (λ = 430 nm) for 60 min. (c) Schematic illustration of photocatalytic water oxidation on the $(Fe,Ru)O_x$-loaded Bi_4TaO_8Cl photocatalyst using Fc^+ as the electron acceptor.

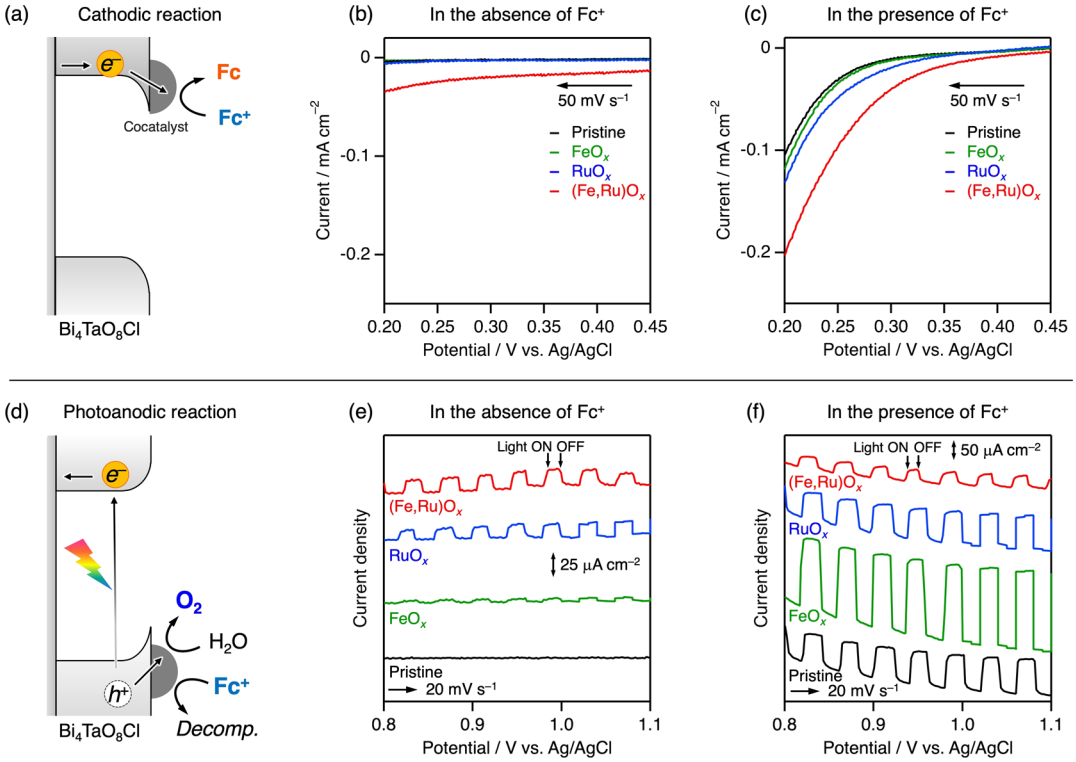

Figure 4. (a) Schematic illustration of cathodic response on an n-type Bi_4TaO_8Cl electrode and (b, c) linear sweep voltammograms of cocatalyst loaded and unloaded Bi_4TaO_8Cl electrodes in the absence (b) and presence (c) of Fc^+ (1 mM) in an aqueous solution containing NaCl solution (0.1 M, pH 2.5 adjusted by HCl) under an Ar atmosphere. (d) Schematic illustration of photoanodic response on an n-type Bi_4TaO_8Cl electrode and (e, f) linear sweep voltammograms of cocatalyst loaded and unloaded Bi_4TaO_8Cl electrodes in an aqueous solution containing NaCl solution (0.1 M, pH 2.5 adjusted by HCl) in the absence (e) and presence (f) of Fc^+ (1 mM) under intermittent visible-light irradiation (λ = 430 nm) under an Ar atmosphere.

https://doi.org/10.1021/jacs.5c02276
J. Am. Chem. Soc. XXXX, XXX, XXX−XXX

RuO_x and $(Fe,Ru)O_x$ species (Figure S16). RuO_x-loaded Bi_4TaO_8Cl had a feature almost identical to that of reference RuO_2 in the Fourier-transformed Ru K edge EXAFS spectrum (Figure S16a). In contrast, a peak corresponding to the second coordination sphere (~3 Å) in Ru K edge EXAFS disappeared in the $(Fe,Ru)O_x$-loaded sample. In addition, the peak features of the first coordination sphere (1 to 2 Å) in Fe K edge EXAFS spectra were slightly but obviously different compared to those of FeO_x and $(Fe,Ru)O_x$ species (Figure S16b). These results suggest the interaction between the Ru and Fe species on the surface of Bi_4TaO_8Cl. The above-described photoelectrochemistry implies a possible role of the Fe species in $(Fe,Ru)O_x$ as a blocker suppressing access to Fc^+ or a trapper of water molecules in a neighborhood of the RuO_x active site, although further investigation is needed to unveil the accurate roles of $(Fe,Ru)O_x$ species.

Z-Schematic Photocatalysis of Organics Conversion Using Water as an Electron Source via Phase-Migrating Ferrocenium/Ferrocene Electron Transportation. The successful photocatalytic water oxidation using Fc^+ as the electron acceptor described above enabled the generation of Fc by using water as an electron source. If Fc can be utilized as the electron donor, then the photoredox catalysis that has required a sacrificial reductant can be converted to a nonsacrificial system using water as an electron source. We chose the reductive coupling of water-insoluble benzyl bromide (Bn-Br), which is a representative model photoredox reaction that has required sacrificial reagents,[36−38] as the initial trial for the photoredox reaction to couple with water oxidation by the Fc^+/Fc redox mediator. As the photoredox catalyst, we employed a molecular iridium complex $[Ir(C6)_2(dmb)](PF_6)$ (C6 = coumarin 6, dmb = 4,4′-dimethyl-2,2′-bipyridine). As shown in Figure 5a, $[Ir(C6)_2(dmb)](PF_6)$ shows strong visible

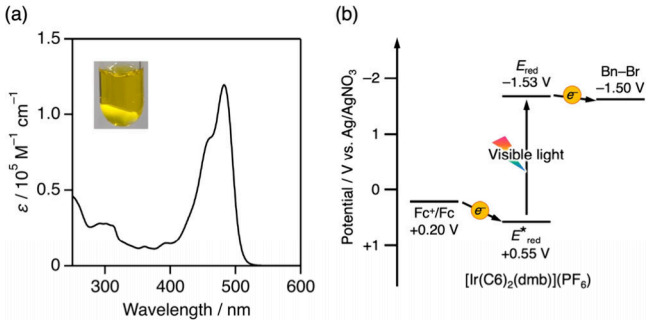

Figure 5. (a) UV−visible absorption spectrum in dichloroethane solution and (b) energy diagram of $[Ir(C6)_2(dmb)](PF_6)$ for photochemically reducing benzyl bromide using Fc as an electron donor.

light absorption at λ_{max} = 482 nm (ε = 119,000 M^{-1} cm^{-1}), which is ascribed to the singlet ligand-centered (^{1}LC) electron transition of a minor contribution of charge transfer transition to the dmb ligand.[39] The excited state of $[Ir(C6)_2(dmb)](PF_6)$ has enough potential (E^*_{red} = 0.55 V vs Ag/$AgNO_3$) to accept an electron from Fc (E_{ox} = 0.20 V) whereas the reduced $[Ir(C6)_2(dmb)](PF_6)$ (E_{red} = −1.53 V) can supply an electron to Bn-Br (−1.50 V) (Figure 5b, see also the Supporting Information, Figures S17−S19 and Table S2, for the details of determining redox potentials in both ground and excited states). The photoinduced electron transfer from Fc to the excited Ir(III) complex, which was evaluated by emission quenching measurements to give a quenching rate constant of 6.7 × 10^9 M^{-1} s^{-1} (Figures S20 and S21), can initiate photoredox catalysis.

In the first step, reductive coupling of benzyl bromide was carried out by visible-light irradiation (λ = 470 nm) of a H_2O/DCE biphasic solution containing $[Ir(C6)_2(dmb)](PF_6)$ (0.05 mM) as a photoredox catalyst, Bn-Br (50 mM), and Fc (10 mM). All of the substrates were selectively distributed in the DCE phase before the reaction (Figure S22). Visible-light irradiation resulted in the formation of dibenzyl (Bn_2) and Fc^+ in the DCE and aqueous phases, respectively (Figures 6a and S23). The molar ratio of generated Bn_2 (5.0 μmol) and Fc^+ (9.9 μmol) was approximately 1:2, which satisfies the redox reaction shown in eq 2.

$$\mathrm{Bn{-}Br + Fc} \xrightarrow{[Ir(C6)_2(dmb)](PF_6)/h\nu\ (=470\ nm)} \frac{1}{2}\mathrm{Bn_2 + Fc^+ + Br^-} \quad (2)$$

In the absence of photoirradiation, $[Ir(C6)_2(dmb)](PF_6)$, Fc, or the aqueous phase, no product was formed (Figures 6b and S24−S27). Notably, the aqueous phase plays an important role in accepting the generated Fc^+, which spontaneously migrates to the aqueous phase because of the drastic change to its partition coefficient from Fc (Figure S22c,e) upon photoinduced electron transfer (Figure 6c). The Fc^+ escaping from the DCE to the aqueous phase enables interphase separation of the charge-separated pair (i.e., $[Ir(C6)_2(dmb)]$ (org.) and Fc^+ (aq.)), which suppresses backward charge recombination ($[Ir(C6)_2(dmb)] + Fc^+ \rightarrow [Ir(C6)_2(dmb)]^+ + Fc$), facilitating the photoredox catalysis in the biphasic solution (Figure 7). Furthermore, the Fc^+ formation rate increased 3.6 times by adding NBu_4Cl (10 mM) to the biphasic solution (Figures 6b and S28). As previously reported for various anions,[26,40] the generated Fc^+ in the DCE phase migrates to the aqueous phase accompanied by an anion (A^-) according to the driving force $\Delta G(Fc^+A^-)_{DCE\rightarrow H_2O}$ as expressed by eq 3.

$$\Delta G(Fc^+A^-)_{DCE\rightarrow H_2O} = \Delta G(Fc^+)_{DCE\rightarrow H_2O} + \Delta G(A^-)_{DCE\rightarrow H_2O} \quad (3)$$

The $\Delta G(Fc^+)_{DCE\rightarrow H_2O}$ was reported to be −2.0 kJ mol^{-1},[41] and the presence of Cl^- ($\Delta G(Cl^-)_{DCE\rightarrow H_2O}$ = −46.4 kJ mol^{-1})[40] in the DCE phase greatly increases the driving force of the phase migration of the Fc^+A^- ion pair. Therefore, the partition equilibrium of Fc^+ shifts to the aqueous phase, resulting in more effective interphase charge separation and efficient Bn_2 formation.

The photocatalytic reductive coupling of benzyl bromide resulted in the partitioning of the Fc^+ in the aqueous phase (Step (I) in Figure 8a) where it was subsequently utilized as the electron acceptor for water oxidation (Step (II) in Figure 8a). $(Fe,Ru)O_x$-loaded Bi_4TaO_8Cl was added to the separated aqueous Fc^+ solution and exposed to visible light (λ = 430 nm). Visible-light irradiation led to the complete consumption of Fc^+ with the formation of O_2 and Fc (Figure S29) at an Fc/O_2 stoichiometric ratio of 4:1 (eq 1). Notably, extraction of the resulting aqueous solution with DCE completely recovered the Fc (10 μmol) used at the starting point of step (I). Eventually, steps (I) and (II) generated Bn_2 and O_2 in a molar ratio of 2:1 (Figure 8b), which satisfied the stoichiometric ratio of the reductive coupling of Bn-Br harnessing water oxidation (Figure 8a, lower). To the best of our knowledge, this is the first

https://doi.org/10.1021/jacs.5c02276
J. Am. Chem. Soc. XXXX, XXX, XXX−XXX

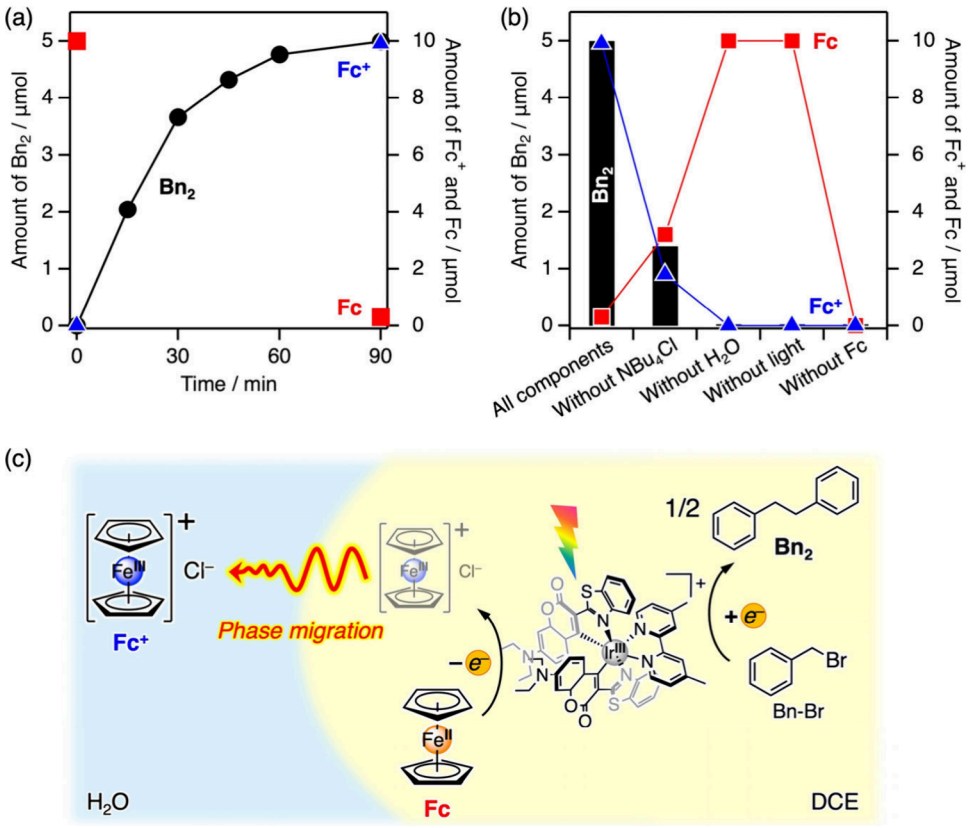

Figure 6. (a) Time course of dibenzyl and Fc^+ formation along with Fc conversion from a biphasic DCE/HCl aq. solution (2:1, v/v; 3.0 mL; pH of the aqueous phase was adjusted to 2.5) containing $[Ir(C6)_2(dmb)](PF_6)$ (0.05 mM), Fc (10 mM), benzyl bromide (50 mM), and NBu_4Cl (10 mM) under visible-light irradiation (λ = 470 nm). (b) Comparison of the photocatalytic activities for Bn_2 and Fc^+ formation as well as Fc conversion depending on the reaction condition. (c) Schematic illustration of the reductive C−C coupling of benzyl bromide catalyzed by the $[Ir(C6)_2(dmb)](PF_6)$ photocatalyst using Fc as a phase-migrating electron donor.

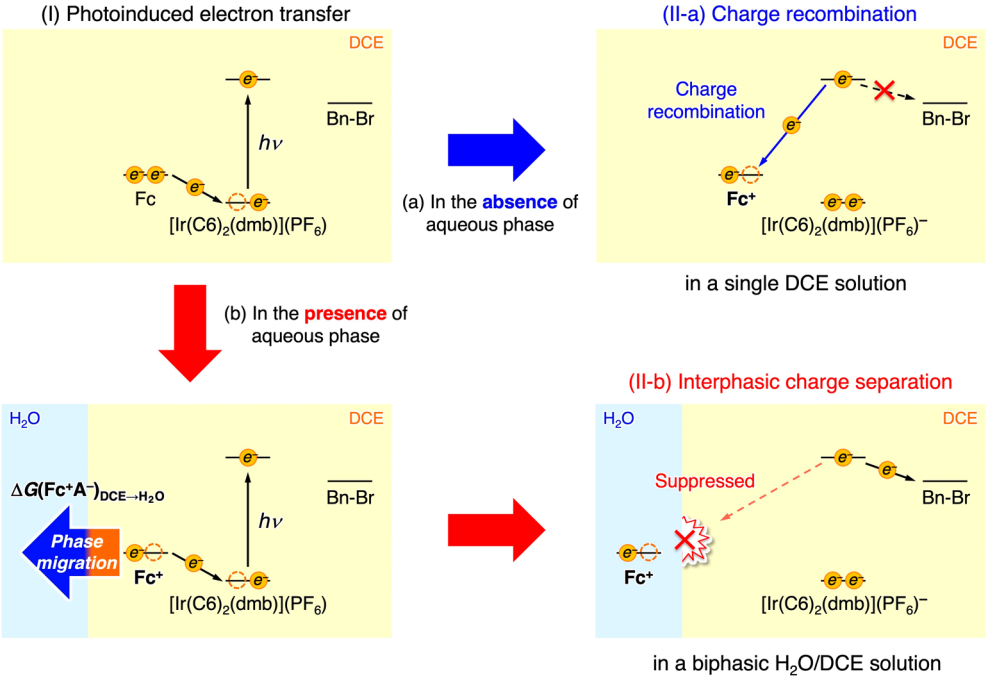

Figure 7. Photoinduced electron transfer and backward charge recombination processes without and with the interphasic migration of Fc^+.

example of Z-scheme photocatalysis that can reduce a "water-insoluble" substrate by using water as an electron source. Importantly, the overall reaction is uphill-type light energy conversion to chemical energy with a positive change in the Gibbs free energy (ΔG = 152.6 kJ mol^{-1}). The light energy conversion efficiency was estimated to be 0.012%.

https://doi.org/10.1021/jacs.5c02276
J. Am. Chem. Soc. XXXX, XXX, XXX−XXX

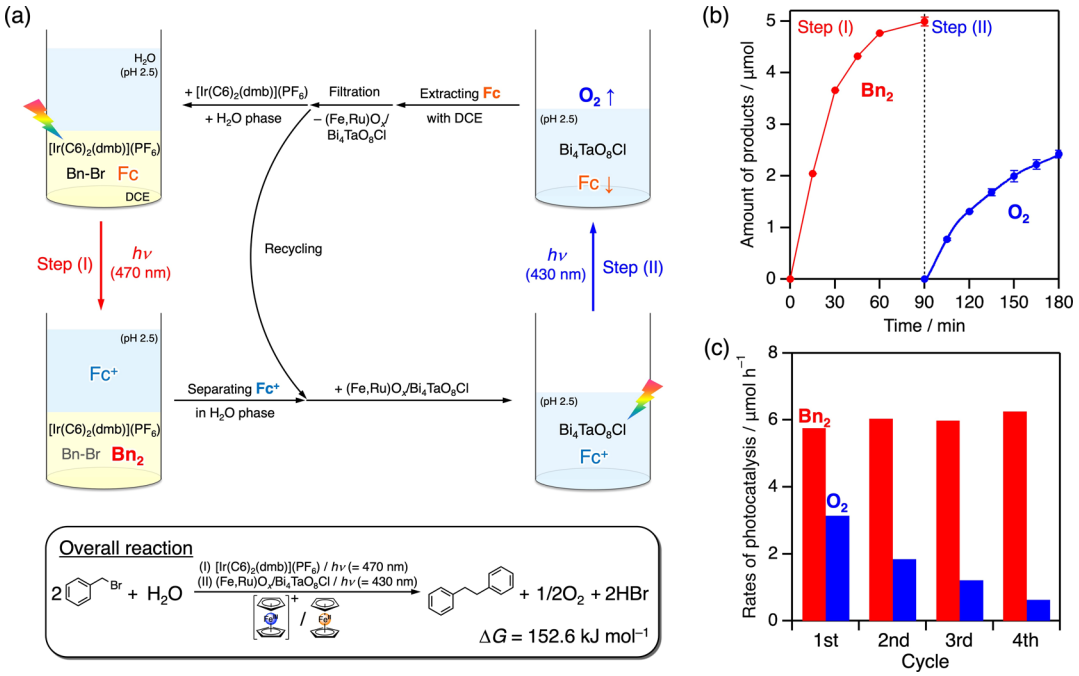

Figure 8. (a) Experimental outline of a step-by-step Z-scheme photocatalytic reaction utilizing Fc^+/Fc as the phase-migrating electron mediator. (b) Time course for the reductive coupling of benzyl bromide (Step (I)) and water oxidation (Step (II)). (c) Rates of repeated step-by-step Z-scheme photocatalytic reactions.

The Z-scheme cycle for the reductive C−C coupling of benzyl bromide could be repeated by using recovered Fc. The turnover numbers of Bn_2 formation were 2.7, 271, and 4.2 based on the Fc, $[Ir(C6)_2(dmb)](PF_6)$, and $(Fe,Ru)O_x$ cocatalyst employed. However, the rate of O_2 evolution decreased gradually with an increasing number of cycles (Figure 8c). A similar deactivation was observed in a repeated half-reaction of the evolution of O_2 with the Fc extraction process with DCE (Figure S30). X-ray photoelectron spectra of $(Fe,Ru)O_x$-loaded Bi_4TaO_8Cl after a cycle of photocatalytic water oxidation (Figure S31) suggested the partial loss of surface FeO_x species and the state closer to RuO_x-loaded Bi_4TaO_8Cl, which has less selectivity for water oxidation (Figure 3b). In fact, the rate of O_2 evolution was maintained when fresh $(Fe,Ru)O_x$-loaded Bi_4TaO_8Cl was employed in the second cycle (Figure S32). Although the dissolution of Fe species as Fe ions in acidic solution (pH < 2.5) has been reported,[1,42] we found the unique stability of $(Fe,Ru)O_x$ species for dissolution in an acidic solution compared with FeO_x species (Table S3). Hence, the dissolution of Fe species in $(Fe,Ru)O_x$ is likely due to treatment with DCE. Stabilization of water-oxidizing cocatalysts is an important challenge for future research.

An integrated (i.e., one-step) overall Z-scheme reaction was also conducted without extraction steps by using a biphasic solution composed of DCE solution containing the Ir(III) complex and Bn-Br and an aqueous solution containing $(Fe,Ru)O_x$-loaded Bi_4TaO_8Cl and Fc^+ (Figure 9). Despite the fact that the reaction was started from Fc^+ in the absence of Fc, the reduction product Bn_2 (0.7 μmol) was generated with a turnover number of 14 (based on the $[Ir(C6)_2(dmb)](PF_6)$ photocatalyst) accompanied by the formation of O_2 (0.1 μmol) (Figure 9a). On the other hand, no Bn_2 or O_2 was formed in the absence of Fc^+. These results clearly indicate the occurrence of water oxidation using Fc^+ as the electron

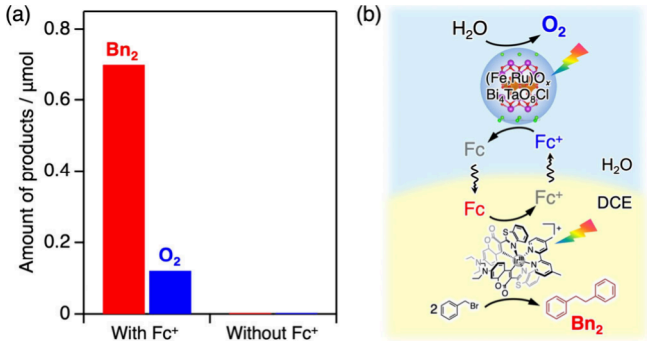

Figure 9. Integrated (one-step) biphasic Z-scheme photocatalysis: (a) Amounts of Bn_2 and O_2 generated after visible-light irradiation for 60 min to a biphasic HCl aq./DCE solution (4 mL; 3:1, v/v; pH of the aqueous phase was adjusted to 2.5) containing $(Fe,Ru)O_x$-loaded Bi_4TaO_8Cl (5 mg), $[Ir(C6)_2(dmb)](PF_6)$ (0.05 mM), Bn-Br (50 mM), and NBu_4Cl (10 mM) in the presence or absence of Fc^+ (2 mM). (b) Schematic illustration of the Z-scheme photocatalysis via phase-migrating electron transportation.

acceptor and generated Fc migrating to the DCE phase to serve as an electron donor for the reductive coupling of Bn-Br (Figure 9b). However, the materials balance of generated Bn_2 (0.7 μmol) and O_2 (0.1 μmol) did not follow the stoichiometry (2:1), possibly due to the occurrence of excessive oxidation of Fc^+ on the semiconductor photocatalyst, as discussed above. The ingenuity of the reaction system to overcome the problem is an important future challenge.

Z-scheme photoredox catalysis was also applicable for the reductive C−C coupling of benzyl bromides with electron-donating or -withdrawing groups on the aromatic ring using water as an electron donor (Figures 10a and S33−S37). This demonstration was further expanded to the hydrogenation of an olefin (dimethyl maleate), which has so far required a sacrificial electron donor,[43,44] using water as an electron source

https://doi.org/10.1021/jacs.5c02276
J. Am. Chem. Soc. XXXX, XXX, XXX−XXX

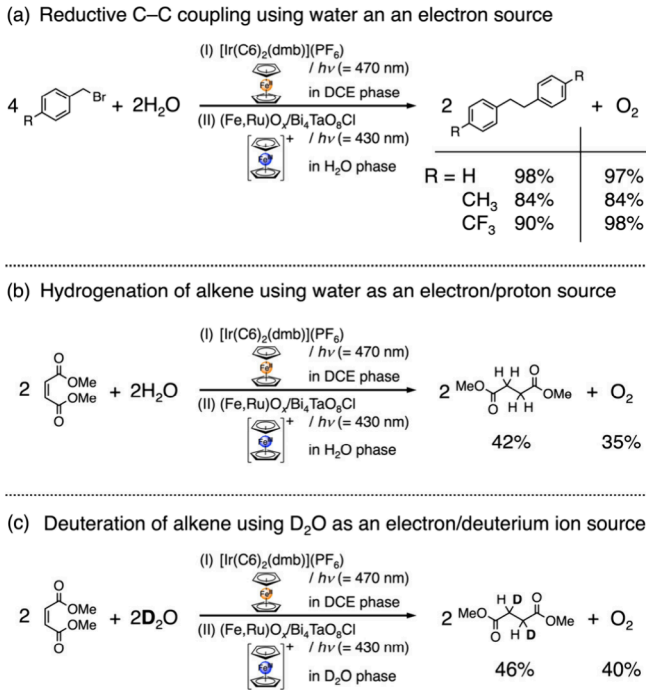

Figure 10. Results of photocatalytic reactions for (a) the reductive coupling of benzyl bromide analogues, (b) hydrogenation, and (c) deuteration of olefins by using water as an electron source. The yield was evaluated based on the added Fc in the initial step and the material balance of the reaction.

(ΔG = +156.9 kJ mol^{-1}) (Figures 10b and S38 and S39). The photocatalytic transformation of dimethyl maleate to dimethyl succinate proceeded in a H_2O/DCE biphasic solution in the same manner as the reductive coupling of benzyl bromides. Although the yield was lower than that in the case of the reductive coupling of benzyl bromides, the formation ratio of dimethyl succinate and Fc^+ was 1:2, satisfying eq 4.

$$\text{dimethyl malate} + 2\text{Fc} + 2\text{H}^+ \xrightarrow{[\text{Ir(C6)}_2\text{(dmb)}](\text{PF}_6)/h\nu\ (=470\ \text{nm})} \text{dimethyl succinate} + 2\text{Fc}^+ \quad (4)$$

Using D_2O instead of H_2O as the aqueous phase, two deuterium atoms were respectively added to the 2,3 carbons in the olefin generating butanedioic-2,3-d_2 acid, dimethyl ester (Figure 10c), as indicated by ^{1}H NMR spectra (Figure S40). Therefore, this reaction is a two-electron/two-proton reduction of an olefin using water as the electron and proton sources. Notably, Fc, which acts as an electron donor in these reactions, was almost quantitatively recycled by water oxidation in all cases (Figures S29, S35, S37, S39, and S41), resulting in the overall reaction being uphill-type light energy conversion to chemical energy with the positive changes in the Gibbs free energy ($\Delta G > 0$) (Figure 10). This is distinct from the conventional photoreduction of organic compounds with the consumption of irreversible sacrificial reductants as waste.

To date, various types of redox mediators such as IO_3^-/I^-,[21] Fe^{3+}/Fe^{2+},[45] VO_2^+/VO^{2+},[46] $[Co(bpy)_3]^{3+/2+}$,[47] $[Fe(CN)_6]^{3-/4-}$,[48] and polyoxometalates[49] have been reported for water splitting into H_2 and O_2. However, these mediators are poorly soluble in organic solutions (e.g., DCE) that are immiscible with water. By simply employing conventional redox mediators, therefore, it is not possible to expand the Z-scheme strategy from H_2 evolution to the conversion of most organic compounds using water as an electron source. In contrast, our strategy opens the door for the reductive conversion of water-insoluble substrates using water as the electron source by a step-by-step Z-scheme via a phase-migrating Fc^+/Fc shuttle redox mediator between immiscible water and DCE solutions.

CONCLUSIONS

We have demonstrated an unconventional Z-scheme system for the photocatalytic conversion of water-insoluble benzyl bromide by using water as the electron source. In a dichloroethane (DCE)/water biphasic solution, the molecular Ir(III) complex acts as a photoredox catalyst for the reductive coupling of benzyl bromide using ferrocene (Fc) as an electron donor in the DCE phase. On the other side, an aqueous dispersion of a Bi_4TaO_8Cl semiconductor loaded with a $(Fe,Ru)O_x$ cocatalyst photocatalyzed water oxidation using ferrocenium (Fc^+) as an electron acceptor. Because the partition coefficients of Fc^+/Fc are significantly different, the Fc^+ and Fc generated by photoinduced electron transfer in each reaction could be selectively extracted to the opposite liquid phase. Spontaneous phase migration enables direction-selective electron transport across the organic/water interface that connects the reduction and oxidation reactions in the separated reaction phase. Finally, photocatalytic reductive conversion of "water-insoluble" organic compounds using water as the electron/proton source was demonstrated through step-by-step Z-scheme photocatalysis with phase-migrating Fc^+/Fc electron transportation. This challenging reaction was achieved by combinational utilization of a heterogeneous semiconductor photocatalyst and a homogeneous molecular photoredox catalyst in a rationally constructed biphasic solution with the phase-migrating electron mediator. This study thus expands the potential of Z-scheme photocatalysis connecting various photocatalyst materials and molecules developed in individual fields for applications in various types of molecular conversions utilizing water as an electron source.

EXPERIMENTAL SECTION

Photocatalytic Reactions. *Photocatalytic Water Oxidation.* An LED lamp (CL-H1-430-9-1-B and CL-H1LCB02, Asahi Spectra Co.) was used as the light source for illumination with visible light (λ = 430 nm). For photocatalytic water oxidation, a suspension of Bi_4TaO_8Cl-based photocatalyst (10 mg) in 5.0 mL of an aqueous Fc^+Cl^- (1 mM, pH 2.5 adjusted with HCl) solution was stirred in a gastight Pyrex cell (20.7 mL), which was sealed with exclusive aluminum cap with butyl/PTFE septum. The reaction suspension was degassed by bubbling it with Ar for 15 min prior to visible-light irradiation. The generated O_2 concentration was monitored using a FireSting Oxygen monitor (PyroScience GmbH) inside the reaction cell (Figure S42a). The minimum air contamination (<0.02 μmol) was confirmed by monitoring O_2 concentrations before and after the photoirradiation. After the photocatalysis of water oxidation, the suspension was transferred to a vial bottle with H_2O (3 × 1.0 mL), and then DCE (2.0 mL) was added to the suspension to extract the Fc. The aqueous reaction solution and DCE extract were filtered and analyzed by UV–visible absorption using a Shimadzu UV-1800 spectrometer in a quartz cell (1 × 10 mm). For control experiments, the same procedure was carried out without each component (Fc^+ or light irradiation). Detailed quantification data, including the calibration curves (Figures S43–S48), are available in the Supporting Information.

Step-by-Step Z-Scheme Photocatalysis. A DCE solution (1 mL) of Fc (10 mM), $[Ir(C6)_2(dmb)](PF_6)$ (0.05 mM), a reduction substrate (50 mM), and NBu_4Cl (10 mM) was placed in a septum-

https://doi.org/10.1021/jacs.5c02276
J. Am. Chem. Soc. XXXX, XXX, XXX–XXX

sealed test tube (inner diameter: 10 mm; volume: 8.4 mL) before water was added (2 mL; pH 2.5 adjusted with HCl) (Figure S42b). The biphasic solution was degassed by bubbling with Ar (10 min) and irradiated at λ = 470 nm using a CL-H1-470-9-1 (Asahi Spectra Co.) with vigorous stirring. The reduction substrates used were benzyl bromide (Bn-Br), 4-methylbenzyl bromide, 4-(trifluoromethyl)benzyl bromide, and dimethyl malate. The products of the aqueous phase (i.e., Fc^+) were analyzed in a quartz cell (1 × 10 mm) by UV−visible absorption spectroscopy using a Shimadzu UV-1800 spectrometer. The products in the DCE phase were analyzed using high-performance liquid chromatography (HPLC) and/or ^{1}H NMR spectroscopy using a JEOL ECX400 spectrometer. HPLC analyses were performed using a Shimadzu LC-20AD system equipped with a Phenomenex column (250 × 4.6 mm^2, 4 mm). A CH_3CN/H_2O (80:20, v/v) solution was used as the eluent at a flow rate of 1.0 mL min^{-1} (column temperature: 313 K), and a Shimadzu SPD-10A was used as the UV−vis detector. Under these analytical conditions, the retention times were determined using purchased or as-prepared samples (Bn-Br: 4.6 min; Fc: 7.0 min; and Bn_2: 9.4 min). After the reduction reaction, Fc^+ in the aqueous phase was collected with aqueous HCl solution (pH 2.5) until the total amount of aqueous solution reached 5.0 mL, and then it was placed in the gastight Pyrex vial containing (Fe,Ru)O_x-loaded Bi_4TaO_8Cl (10 mg). Photocatalytic water oxidation was performed in the same manner as that described above. For the repeated Z-scheme photocatalysis, the Fc generated by photocatalytic water oxidation was extracted with DCE solution (1 mL) containing $[Ir(C6)_2(dmb)](PF_6)$ (0.05 mM), Bn-Br (50 mM), and NBu_4Cl (10 mM), and water (2 mL; pH 2.5 adjusted with HCl) was added in a septum-sealed test tube (inner diameter: 10 mm; volume: 8.4 mL). Multiple cycles of Z-scheme photocatalysis were carried out by repeating the procedure described above. Detailed quantification data, including the calibration curves (Figures S43−S48), are available in the Supporting Information.

Integrated (One-Step) Z-Scheme Photocatalysis. A dichloroethane solution (1 mL) of $[Ir(C6)_2(dmb)](PF_6)$ (0.05 mM), Bn-Br (50 mM), and NBu_4Cl (10 mM) was placed in a septum-sealed test tube (inner diameter: 10 mm; volume: 8.4 mL) before an aqueous dispersion containing (Fe,Ru)O_x-loaded Bi_4TaO_8Cl (5 mg) and Fc^+Cl^- (2 mM) was added (3 mL; pH 2.5 adjusted with HCl). The biphasic solution was degassed by bubbling with Ar (10 min) and irradiated at λ = 430 and 470 nm with stirring (Figure S49).

■ ASSOCIATED CONTENT

Supporting Information

The Supporting Information is available free of charge at https://pubs.acs.org/doi/10.1021/jacs.5c02276.

Experimental details, including synthesis, characterization, determination of photoinduced electron transfer, and photocatalytic reactions (PDF)

■ AUTHOR INFORMATION

Corresponding Authors

Akinobu Nakada − *Department of Energy and Hydrocarbon Chemistry, Graduate School of Engineering, Kyoto University, Nishikyo-ku, Kyoto 615-8510, Japan; Precursory Research for Embryonic Science and Technology (PRESTO), Japan Science and Technology Agency (JST), Kawaguchi, Saitama 332-0012, Japan;* orcid.org/0000-0001-6670-5044; Email: nakada@scl.kyoto-u.ac.jp

Ho-Chol Chang − *Department of Applied Chemistry, Faculty of Science and Engineering, Chuo University, Bunkyo-ku, Tokyo 112-8551, Japan;* orcid.org/0000-0001-5159-2737; Email: chang@kc.chuo-u.ac.jp

Ryu Abe − *Department of Energy and Hydrocarbon Chemistry, Graduate School of Engineering, Kyoto University, Nishikyo-ku, Kyoto 615-8510, Japan;* orcid.org/0000-0001-8592-076X; Email: ryu-abe@scl.kyoto-u.ac.jp

Authors

Ren Itagaki − *Department of Energy and Hydrocarbon Chemistry, Graduate School of Engineering, Kyoto University, Nishikyo-ku, Kyoto 615-8510, Japan*

Hajime Suzuki − *Department of Energy and Hydrocarbon Chemistry, Graduate School of Engineering, Kyoto University, Nishikyo-ku, Kyoto 615-8510, Japan;* orcid.org/0000-0002-8891-2033

Osamu Tomita − *Department of Energy and Hydrocarbon Chemistry, Graduate School of Engineering, Kyoto University, Nishikyo-ku, Kyoto 615-8510, Japan;* orcid.org/0000-0002-5910-8732

Complete contact information is available at: https://pubs.acs.org/10.1021/jacs.5c02276

Notes

The authors declare no competing financial interest.

■ ACKNOWLEDGMENTS

This work was supported by JSPS KAKENHI grants (JP24K01603 and JP22K14769), a Grant-in-Aid for Transformative Research Area "Concerto Photocatalysis" (JP23H03830 and JP23H03832), and a JST PRESTO grant JPMJPR20T5 (Controlled Reaction). R.I. acknowledges the support from the JSPS Fellowship for Young Scientists (JP23KJ1351). H.-C.C. acknowledges the financial support from the Research Promotion Fund from the Promotion and Mutual Aid Corporation for Private Schools of Japan.

■ REFERENCES

(1) Wang, Y.; Suzuki, H.; Xie, J.; Tomita, O.; Martin, D. J.; Higashi, M.; Kong, D.; Abe, R.; Tang, J. Mimicking Natural Photosynthesis: Solar to Renewable H_2 Fuel Synthesis by Z-Scheme Water Splitting Systems. *Chem. Rev.* **2018**, *118*, 5201−5241.

(2) Kudo, A.; Miseki, Y. Heterogeneous photocatalyst materials for water splitting. *Chem. Soc. Rev.* **2009**, *38*, 253−278.

(3) Wang, Q.; Domen, K. Particulate Photocatalysts for Light-Driven Water Splitting: Mechanisms, Challenges, and Design Strategies. *Chem. Rev.* **2020**, *120*, 919−985.

(4) Tao, X.; Zhao, Y.; Wang, S.; Li, C.; Li, R. Recent advances and perspectives for solar-driven water splitting using particulate photocatalysts. *Chem. Soc. Rev.* **2022**, *51*, 3561−3608.

(5) Yamazaki, Y.; Takeda, H.; Ishitani, O. Photocatalytic reduction of CO_2 using metal complexes. *J. Photochem. Photobiol. C* **2015**, *25*, 106−137.

(6) Elgrishi, N.; Chambers, M. B.; Wang, X.; Fontecave, M. Molecular polypyridine-based metal complexes as catalysts for the reduction of CO_2. *Chem. Soc. Rev.* **2017**, *46*, 761−796.

(7) Dalle, K. E.; Warnan, J.; Leung, J. J.; Reuillard, B.; Karmel, I. S.; Reisner, E. Electro- and Solar-Driven Fuel Synthesis with First Row Transition Metal Complexes. *Chem. Rev.* **2019**, *119*, 2752−2875.

(8) Li, X.; Yu, J.; Jaroniec, M.; Chen, X. Cocatalysts for Selective Photoreduction of CO_2 into Solar Fuels. *Chem. Rev.* **2019**, *119*, 3962−4179.

(9) Nakada, A.; Kumagai, H.; Robert, M.; Ishitani, O.; Maeda, K. Molecule/Semiconductor Hybrid Materials for Visible-Light CO_2 Reduction: Design Principles and Interfacial Engineering. *Acc. Mater. Res.* **2021**, *2*, 458−470.

(10) Prier, C. K.; Rankic, D. A.; MacMillan, D. W. C. Visible light photoredox catalysis with transition metal complexes: Applications in organic synthesis. *Chem. Rev.* **2013**, *113*, 5322−5363.

(11) Romero, N. A.; Nicewicz, D. A. Organic Photoredox Catalysis. *Chem. Rev.* **2016**, *116*, 10075−10166.

(12) Skubi, K. L.; Blum, T. R.; Yoon, T. P. Dual Catalysis Strategies in Photochemical Synthesis. *Chem. Rev.* **2016**, *116*, 10035−10074.
(13) Chan, A. Y.; Perry, I. B.; Bissonnette, N. B.; Buksh, B. F.; Edwards, G. A.; Frye, L. I.; Garry, O. L.; Lavagnino, M. N.; Li, B. X.; Liang, Y.; et al. Metallaphotoredox: The Merger of Photoredox and Transition Metal Catalysis. *Chem. Rev.* **2022**, *122*, 1485−1542.
(14) Cheung, K. P. S.; Sarkar, S.; Gevorgyan, V. Visible Light-Induced Transition Metal Catalysis. *Chem. Rev.* **2022**, *122*, 1543−1625.
(15) Sheldon, R. A.; Brady, D. Green Chemistry, Biocatalysis, and the Chemical Industry of the Future. *ChemSusChem* **2022**, *15*, No. e202102628.
(16) Suzuki, T. M.; Yoshino, S.; Takayama, T.; Iwase, A.; Kudo, A.; Morikawa, T. Z-Schematic and visible-light-driven CO_2 reduction using H_2O as an electron donor by a particulate mixture of a Ru-complex/$(CuGa)_{1-x}Zn_{2x}S_2$ hybrid catalyst, $BiVO_4$ and an electron mediator. *Chem. Commun.* **2018**, *54*, 10199−10202.
(17) Shaw, M. H.; Twilton, J.; MacMillan, D. W. Photoredox Catalysis in Organic Chemistry. *J. Org. Chem.* **2016**, *81*, 6898−6926.
(18) Mills, A.; Hunte, S. L. An overview of semiconductor photocatalysis. *J. Photochem. Photobiol., A* **1997**, *108*, 1−35.
(19) Chen, D.; Cheng, Y.; Zhou, N.; Chen, P.; Wang, Y.; Li, K.; Huo, S.; Cheng, P.; Peng, P.; Zhang, R.; Wang, L.; Liu, H.; Liu, Y.; Ruan, R. Photocatalytic degradation of organic pollutants using TiO_2-based photocatalysts: A review. *J. Clean. Prod.* **2020**, *268*, 121725.
(20) Zhang, S.; Li, B.; Wang, X.; Zhao, G.; Hu, B.; Lu, Z.; Wen, T.; Chen, J.; Wang, X. Recent developments of two-dimensional graphene-based composites in visible-light photocatalysis for eliminating persistent organic pollutants from wastewater. *Chem. Eng. J.* **2020**, *390*, 124642.
(21) Abe, R.; Sayama, K.; Sugihara, H. Development of new photocatalytic water splitting into H_2 and O_2 using two different semiconductor photocatalysts and a shuttle redox mediator IO_3^-/I^-. *J. Phys. Chem. B* **2005**, *109*, 16052−16061.
(22) Vannoy, K. J.; Edwards, M. Q.; Renault, C.; Dick, J. E. An Electrochemical Perspective on Reaction Acceleration in Microdroplets. *Annu. Rev. Anal. Chem.* **2024**, *17*, 149−171.
(23) Pendergast, A. D.; Gutierrez-Portocarrero, S.; Noriega, R.; White, H. S. Electrical Double Layer Spillover Drives Coupled Electron- and Phase-Transfer Reactions at Electrode/Toluene/Water Three-Phase Interfaces. *J. Am. Chem. Soc.* **2024**, *146*, 30464−30473.
(24) Hong, Y. H.; Lee, Y. M.; Nam, W.; Fukuzumi, S. Molecular Photocatalytic Water Splitting by Mimicking Photosystems I and II. *J. Am. Chem. Soc.* **2022**, *144*, 695−700.
(25) Goren, Z.; Willner, I. Photochemical and chemical reduction of vicinal dibromides via phase transfer of 4,4'-bipyridinium radical: the role of radical disproportionation. *J. Am. Chem. Soc.* **1983**, *105*, 7764−7765.
(26) Itagaki, R.; Takizawa, S.; Chang, H.-C.; Nakada, A. Light-induced electron transfer/phase migration of a redox mediator for photocatalytic C-C coupling in a biphasic solution. *Dalton Trans.* **2022**, *51*, 9467−9476.
(27) Ikeda, S.; Hirao, K.; Ishino, S.; Matsumura, M.; Ohtani, B. Preparation of platinized strontium titanate covered with hollow silica and its activity for overall water splitting in a novel phase-boundary photocatalytic system. *Catal. Today* **2006**, *117*, 343−349.
(28) Kunioku, H.; Higashi, M.; Tomita, O.; Yabuuchi, M.; Kato, D.; Fujito, H.; Kageyama, H.; Abe, R. Strong hybridization between Bi-6s and O-2p orbitals in Sillén-Aurivillius perovskite Bi_4MO_8X (M = Nb, Ta; X = Cl, Br), visible light photocatalysts enabling stable water oxidation. *J. Mater. Chem. A* **2018**, *6*, 3100−3107.
(29) Ogawa, K.; Nakada, A.; Suzuki, H.; Tomita, O.; Higashi, M.; Saeki, A.; Kageyama, H.; Abe, R. Flux Synthesis of Layered Oxyhalide Bi_4NbO_8Cl Photocatalyst for Efficient Z-Scheme Water Splitting under Visible Light. *ACS Appl. Mater. Interfaces* **2019**, *11*, 5642−5650.
(30) Nakada, A.; Suzuki, H.; Vequizo, J. J. M.; Ogawa, K.; Higashi, M.; Saeki, A.; Yamakata, A.; Kageyama, H.; Abe, R. Fe/Ru Oxide as Versatile and Effective Cocatalyst for Boosting Z-Scheme Water Splitting: Suppressing Undesirable Backward Electron Transfer. *ACS Appl. Mater. Interfaces* **2019**, *11*, 45606−45611.
(31) Suzuki, H.; Kunioku, H.; Higashi, M.; Tomita, O.; Kato, D.; Kageyama, H.; Abe, R. Lead Bismuth Oxyhalides $PbBiO_2X$ (X = Cl, Br) as Visible-Light-Responsive Photocatalysts for Water Oxidation: Role of Lone-Pair Electrons in Valence Band Engineering. *Chem. Mater.* **2018**, *30*, 5862−5869.
(32) Murofushi, K.; Ogawa, K.; Suzuki, H.; Sakamoto, R.; Tomita, O.; Kato, K.; Yamakata, A.; Saeki, A.; Abe, R. Earth-abundant iron(III) species serves as a cocatalyst boosting the multielectron reduction of IO_3^-/I^- redox shuttle in Z-scheme photocatalytic water splitting. *J. Mater. Chem. A* **2021**, *9*, 11718−11725.
(33) Maeda, K.; Abe, R.; Domen, K. Role and Function of Ruthenium Species as Promoters with TaON-Based Photocatalysts for Oxygen Evolution in Two-Step Water Splitting under Visible Light. *J. Phys. Chem. C* **2011**, *115*, 3057−3064.
(34) Nakada, A.; Nishioka, S.; Vequizo, J. J. M.; Muraoka, K.; Kanazawa, T.; Yamakata, A.; Nozawa, S.; Kumagai, H.; Adachi, S.-i.; Ishitani, O.; et al. Solar-driven Z-scheme water splitting using tantalum/nitrogen co-doped rutile titania nanorod as an oxygen evolution photocatalyst. *J. Mater. Chem. A* **2017**, *5*, 11710−11719.
(35) Suzuki, H.; Nitta, S.; Tomita, O.; Higashi, M.; Abe, R. Highly Dispersed RuO_2 Hydrates Prepared via Simple Adsorption as Efficient Cocatalysts for Visible-Light-Driven Z-Scheme Water Splitting with an IO_3^-/I^- Redox Mediator. *ACS Catal.* **2017**, *7*, 4336−4336.
(36) Hironaka, K.; Fukuzumi, S.; Tanaka, T. Tris(bipyridyl)-ruthenium(II)-photosensitized reaction of 1-benzyl-1,4-dihydronicotinamide with benzyl bromide. *J. Chem. Soc. Perkin Trans. 2* **1984**, 1705−1709.
(37) Yu, D.; To, W. P.; Tong, G. S. M.; Wu, L. L.; Chan, K. T.; Du, L.; Phillips, D. L.; Liu, Y.; Che, C. M. Luminescent tungsten(VI) complexes as photocatalysts for light-driven C-C and C-B bond formation reactions. *Chem. Sci.* **2020**, *11*, 6370−6382.
(38) Zhang, Y.; Lee, T. S.; Petersen, J. L.; Milsmann, C. A Zirconium Photosensitizer with a Long-Lived Excited State: Mechanistic Insight into Photoinduced Single-Electron Transfer. *J. Am. Chem. Soc.* **2018**, *140*, 5934−5947.
(39) Takizawa, S.; Ikuta, N.; Zeng, F.; Komaru, S.; Sebata, S.; Murata, S. Impact of Substituents on Excited-State and Photosensitizing Properties in Cationic Iridium(III) Complexes with Ligands of Coumarin 6. *Inorg. Chem.* **2016**, *55*, 8723−8735.
(40) Marcus, Y. Thermodynamic functions of transfer of single ions from water to nonaqueous and mixed solvents: Part I - Gibbs free energies of transfer to nonaqueous solvents. *Pure Appl. Chem.* **1983**, *55*, 977−1021.
(41) Hanzlik, J.; Samec, Z.; Hovorka, J. Transfer of ferricenium cation across water/organic solvent interfaces. *J. Electroanal. Chem.* **1987**, *216*, 303−308.
(42) Pourbaix, M. *Atlas of Electrochemical Equilibria in Aqueous Solutions*, 2nd ed.; National Association of Corrosion Engineers, 1974.
(43) Pac, C.; Ihama, M.; Yasuda, M.; Miyauchi, Y.; Sakurai, H. $Ru(bpy)_3^{2+}$-mediated photoreduction of olefins with 1-benzyl-1,4-dihydronicotinamide: a mechanistic probe for electron-transfer reactions of NAD(P)H-model compounds. *J. Am. Chem. Soc.* **1981**, *103*, 6495−6497.
(44) Zhang, Y.; Petersen, J. L.; Milsmann, C. A Luminescent Zirconium(IV) Complex as a Molecular Photosensitizer for Visible Light Photoredox Catalysis. *J. Am. Chem. Soc.* **2016**, *138*, 13115−13118.
(45) Kato, H.; Hori, M.; Konta, R.; Shimodaira, Y.; Kudo, A. Construction of Z-scheme Type Heterogeneous Photocatalysis Systems for Water Splitting into H_2 and O_2 under Visible Light Irradiation. *Chem. Lett.* **2004**, *33*, 1348−1349.
(46) Miseki, Y.; Fujiyoshi, S.; Gunji, T.; Sayama, K. Photocatalytic Z-Scheme Water Splitting for Independent H_2/O_2 Production via a Stepwise Operation Employing a Vanadate Redox Mediator under Visible Light. *J. Phys. Chem. C* **2017**, *121*, 9691−9697.
(47) Sasaki, Y.; Kato, H.; Kudo, A. $[Co(bpy)_3]^{3+/2+}$ and $[Co(phen)_3]^{3+/2+}$ electron mediators for overall water splitting under

https://doi.org/10.1021/jacs.5c02276
J. Am. Chem. Soc. XXXX, XXX, XXX−XXX

sunlight irradiation using Z-scheme photocatalyst system. *J. Am. Chem. Soc.* **2013**, *135*, 5441−5449.
(48) Shirakawa, T.; Higashi, M.; Tomita, O.; Abe, R. Surface-modified metal sulfides as stable H_2-evolving photocatalysts in Z-scheme water splitting with a $[Fe(CN)_6]^{3-/4-}$ redox mediator under visible-light irradiation. *Sustain. Energy Fuels* **2017**, *1*, 1065−1073.
(49) Tsuji, K.; Tomita, O.; Higashi, M.; Abe, R. Manganese-Substituted Polyoxometalate as an Effective Shuttle Redox Mediator in Z-Scheme Water Splitting under Visible Light. *ChemSusChem* **2016**, *9*, 2201−2208.

https://doi.org/10.1021/jacs.5c02276
J. Am. Chem. Soc. XXXX, XXX, XXX−XXX